Supporting Information for:

"Morphology control of single crystal InSb nanostructures by tuning the growth parameters"

Isha Verma[1], Valentina Zannier[1*], Francesca Rossi[2], Daniele Ercolani[1], Fabio Beltram[1] and Lucia Sorba[1]

[1] NEST, Istituto Nanoscienze- CNR and Scuola Normale Superiore, Piazza San Silvestro 12, I-56127 Pisa, Italy
[2] IMEM-CNR, Parco Area delle Scienze 37/A, I-43124 Parma, Italy

Contents

*correspondence email: valentina.zannier@nano.cnr.it

S1. Distribution of asymmetric InAs/InSb NWs on the as-grown sample

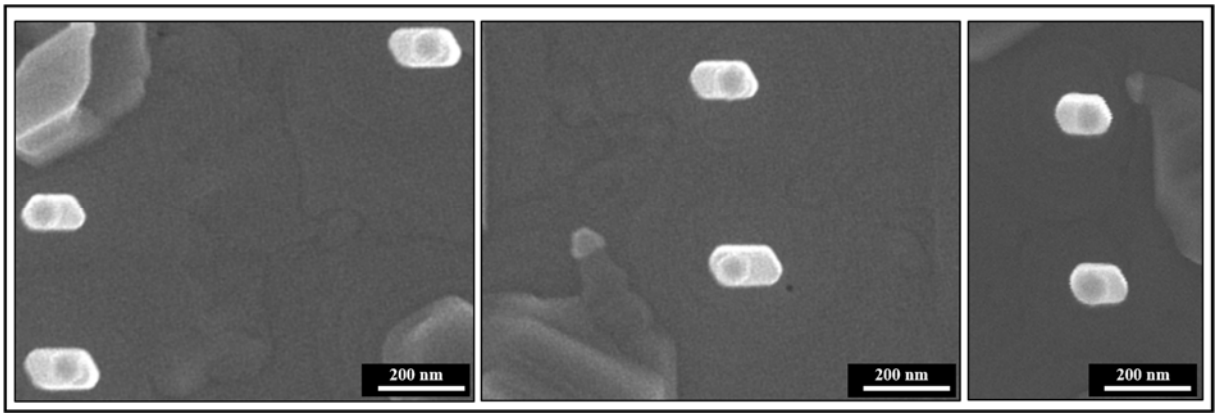

Figure S1. Top view SEM images of asymmetric InAs/InSb NWs recorded from different parts of the substrate. The substrate orientation is the same in all images.

Figure S1 shows top view SEM images of asymmetric InAs/InSb NWs taken from different parts of the same as grown sample. It is clear that all the NWs elongate in the same direction. However, it should be noticed that the final position of the Au NP is not the same for all the asymmetric NWs. As a matter of fact, few NWs show the NP aligned with the InAs stem position, few others show the NP on the opposite side and the vast majority have the NP somewhere in between the two far ends of the asymmetric NWs. The random distribution of the NP on the tip suggests that the NP can unpin from the flat top facet and wet the inclined sidewalls of the NWs, similarly to what reported in ref [9] of the main text.

S2. Yield of InSb Nanoflags

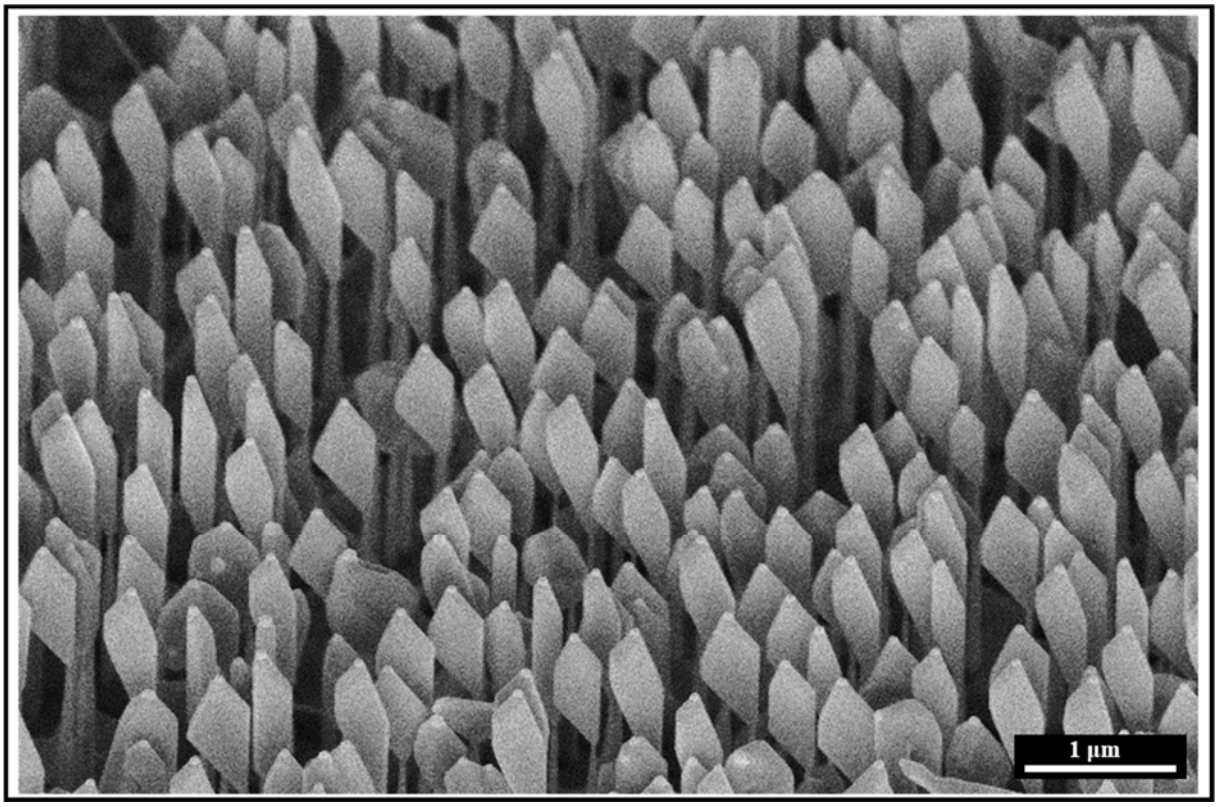

Figure S2. Low magnification 45° tilted SEM image of InSb NFs.

The low magnification SEM image of as grown InSb NFs sample demonstrates the high yield and the general morphology. It should be noted that also in this case the direction of elongation of all the NFs is same. However, NFs with different aperture angle and/or number of side facets are simultaneously obtained.

S3. Statistics on aperture angle of InSb NFs

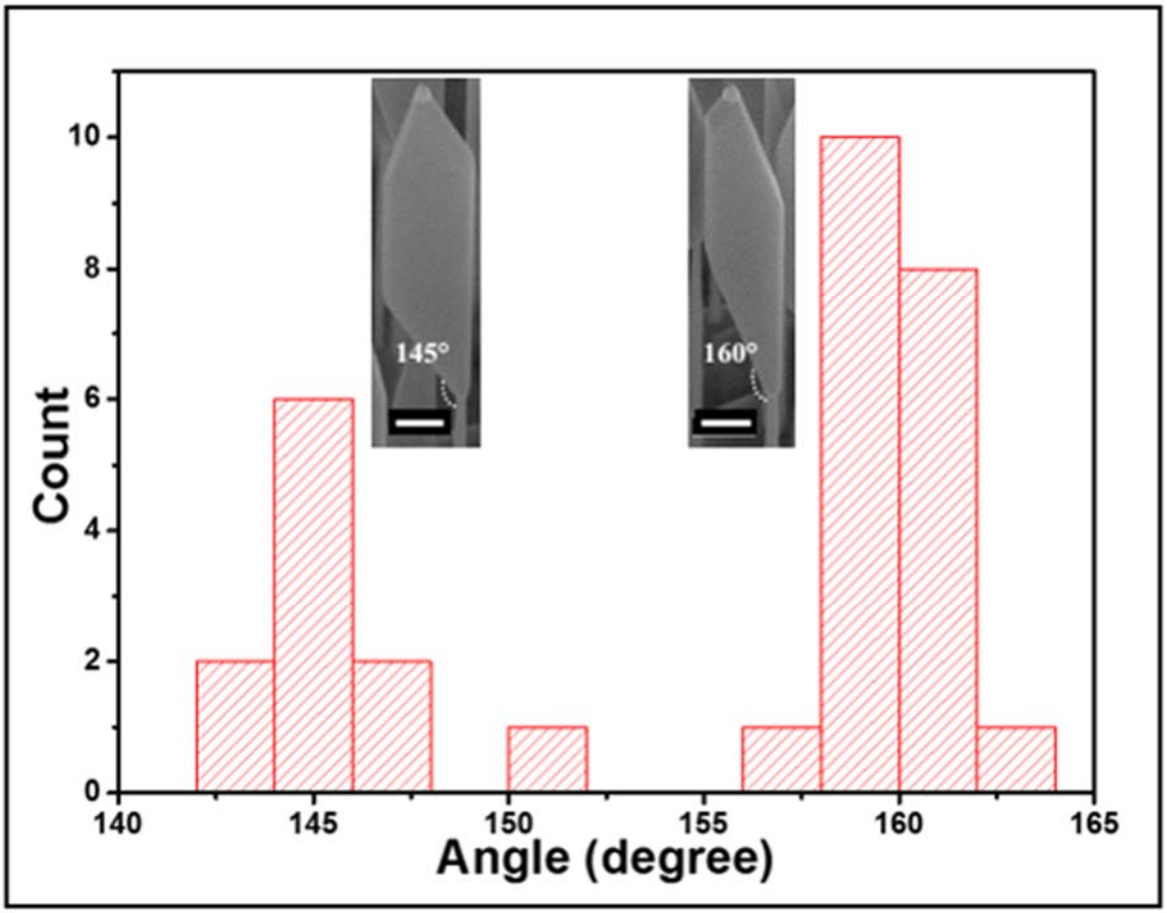

Figure S3. Distribution of InSb NFs with aperture angle of 145° and 160°. Insets show NFs with aperture angle of 145° (left) and 160° (right). The scale bar is 200 nm.

The aperture angle is the angle formed by the NF base facet and the InAs stem. To measure it, the NFs were detached from the substrate and laid flat in a viewing direction perpendicular to the major {-101} facets. The aperture angles are confirmed from HRTEM images. It was found that the distribution is bimodal and the population of the two families one with aperture angle 145° and other with 160° is close to 40:60.

S4. Evolution of NF morphology

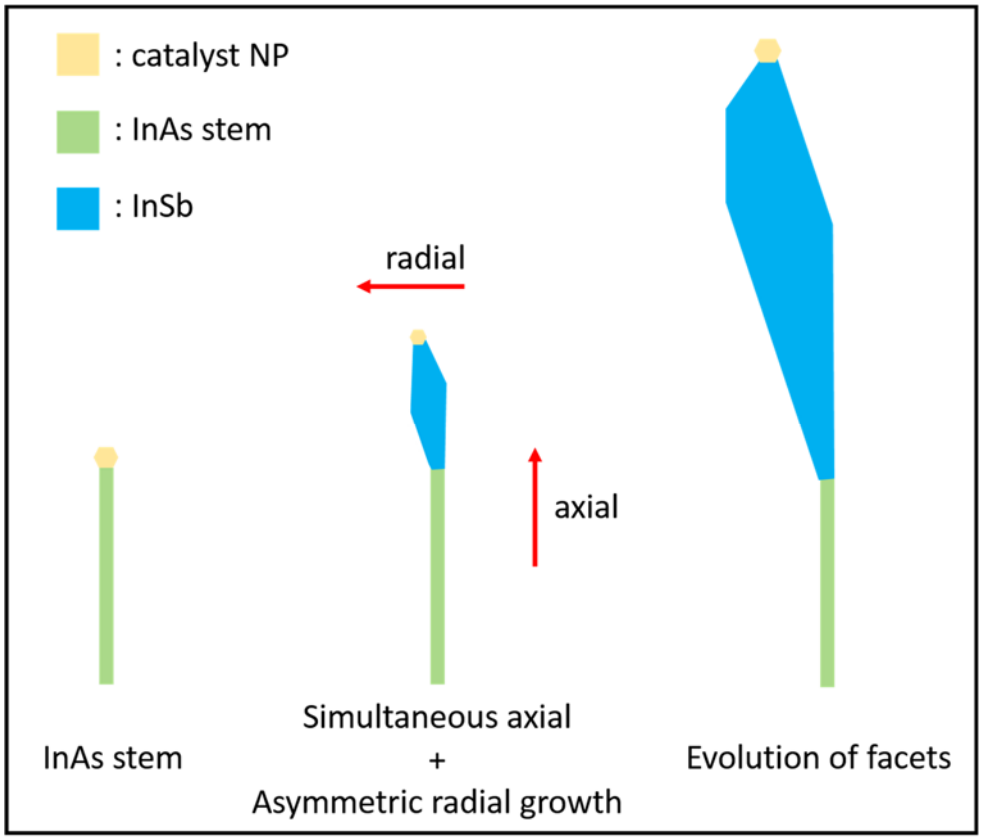

Figure S4. Schematic evolution of NF morphology, considering the two growth mechanisms that simultaneously occur.

As mentioned in the main text, the InSb NF final shape arises from the two growth mechanisms that simultaneously occur: the VLS axial growth on top of the InAs stem and the asymmetric VS radial growth due to stopping the sample rotation that causes the different growth rate on the different sidewalls. A similar interplay between these growth mechanisms is shown in D Pan et al. [ref 8 of the main text], in order to explain the final morphology of InSb NFs grown with Ag catalyst particles. Moreover, the catalyst nanoparticle can unpin from the (111) top facet and wet the inclined facets developed at top part of InSb NF, probably due to comparable surface energies, as already discussed in S1. A similar mechanism has been observed also in María de la Mata et al. [ref 9 of the main text]. We believe that this NP dynamics determines the final InSb NF shape and the final NP position.

S5. Five-sided InSb NF

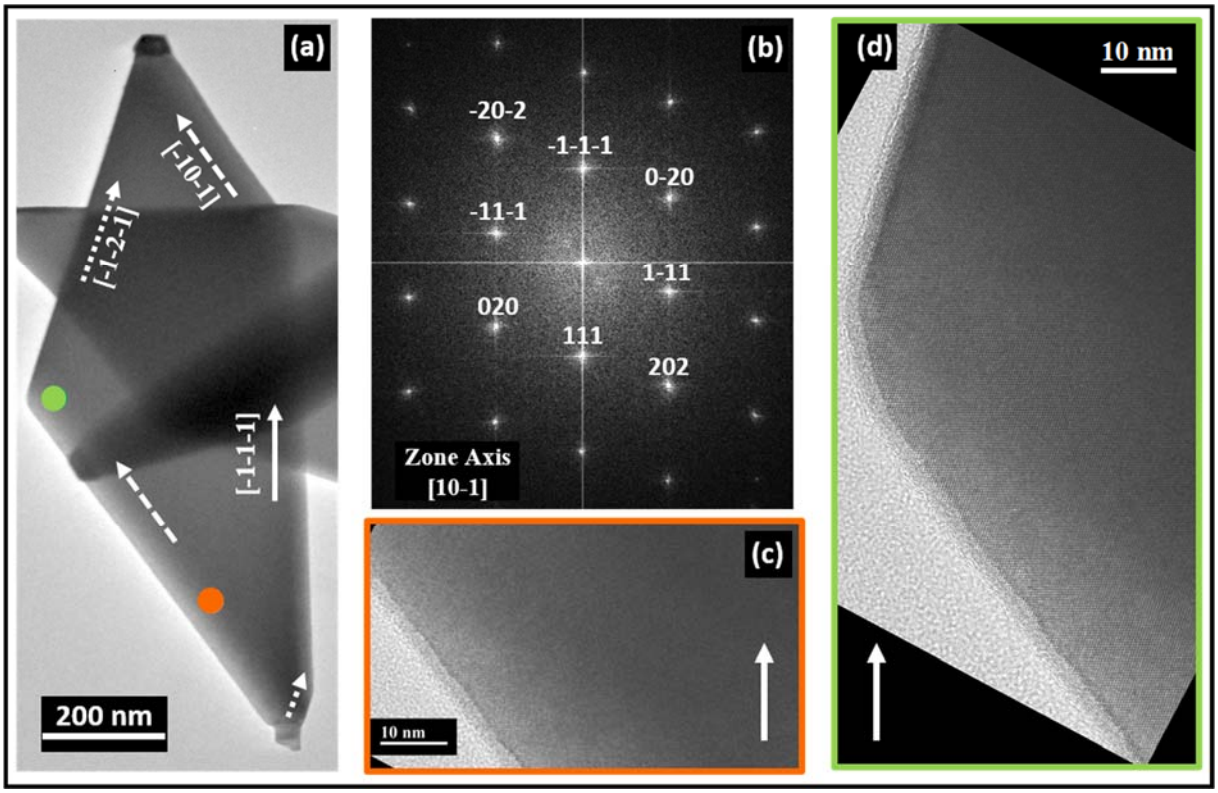

Figure S5. Shape and crystal structure of a 5-sided InSb NF obtained in the same as-grown sample. (a) Low magnification TEM image. The arrows indicate the [-1-1-1] growth direction and the directions of the other flake sides. (b) Corresponding fast Fourier transform acquired along [10-1] zone axis. (c, d) HRTEM images of the lower lateral facet (orange region) and left corner (green region).

Figure S5 shows the TEM images of a 5-sided InSb NF obtained in the same as grown sample, depicted in Fig. S2. The analysis confirms that also 5-sided NFs, as the 6-sided NFs, have a pure zinc blend (ZB) crystal structure free from stacking faults or twinning defects.

S6. Strain analysis

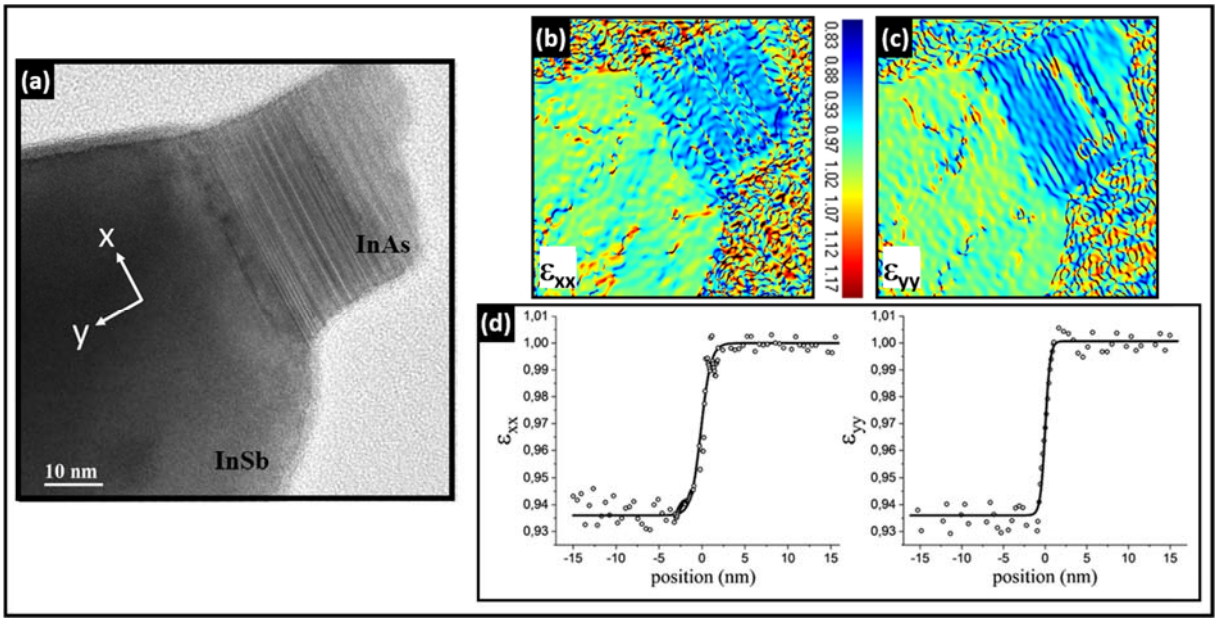

Figure S6. Strain analysis. (a) HR-TEM image of InAs/InSb interface region of the NF. GPA maps of strain component (b) Ɛxx and (c) Ɛyy. (d) Line profile of Ɛxx and Ɛyy.

We evaluated the strain relaxation at the InAs/InSb interface in the NFs. For detailed analysis at the heterointerface, the acquired HR-TEM image (panel (a) of Figure S5) was processed with the geometric phase analysis (GPA) method to extract the in-plane and out-of-plane strain components denoted by Ɛxx and Ɛyy respectively. Panels (b) and (c) correspond to GPA maps of Ɛxx (i.e. variation of the interplanar spacing in the <121> direction) and Ɛyy (i.e. variation of the interplanar spacing in the <111> direction). Panel (d) shows the averaged line profile of Ɛxx and Ɛyy across the InAs/ InSb heterointerface, respectively. A step-like change from about 0.936 (InAs) to 1.000 (InSb) for Ɛxx and Ɛyy is observed, consistently with the 6.4% lattice mismatch between the two materials.

S7. Electron diffraction pattern of the InSb NFs with different aperture angle

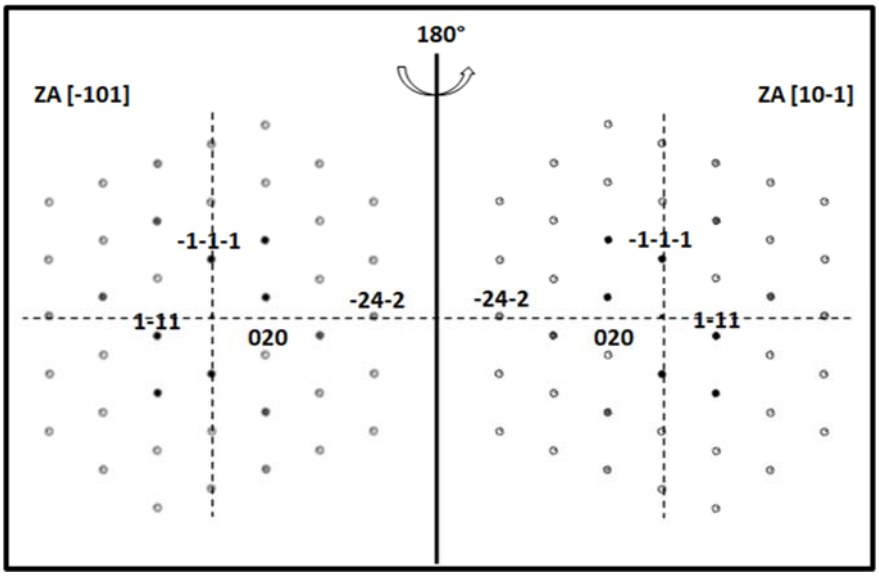

Figure S7. Schematic of the electron diffraction patterns in <-101> zone axis of the InSb NFs with aperture angle of 160° (left) and 145° (right).

S8. 3D atomic model of InSb NFs

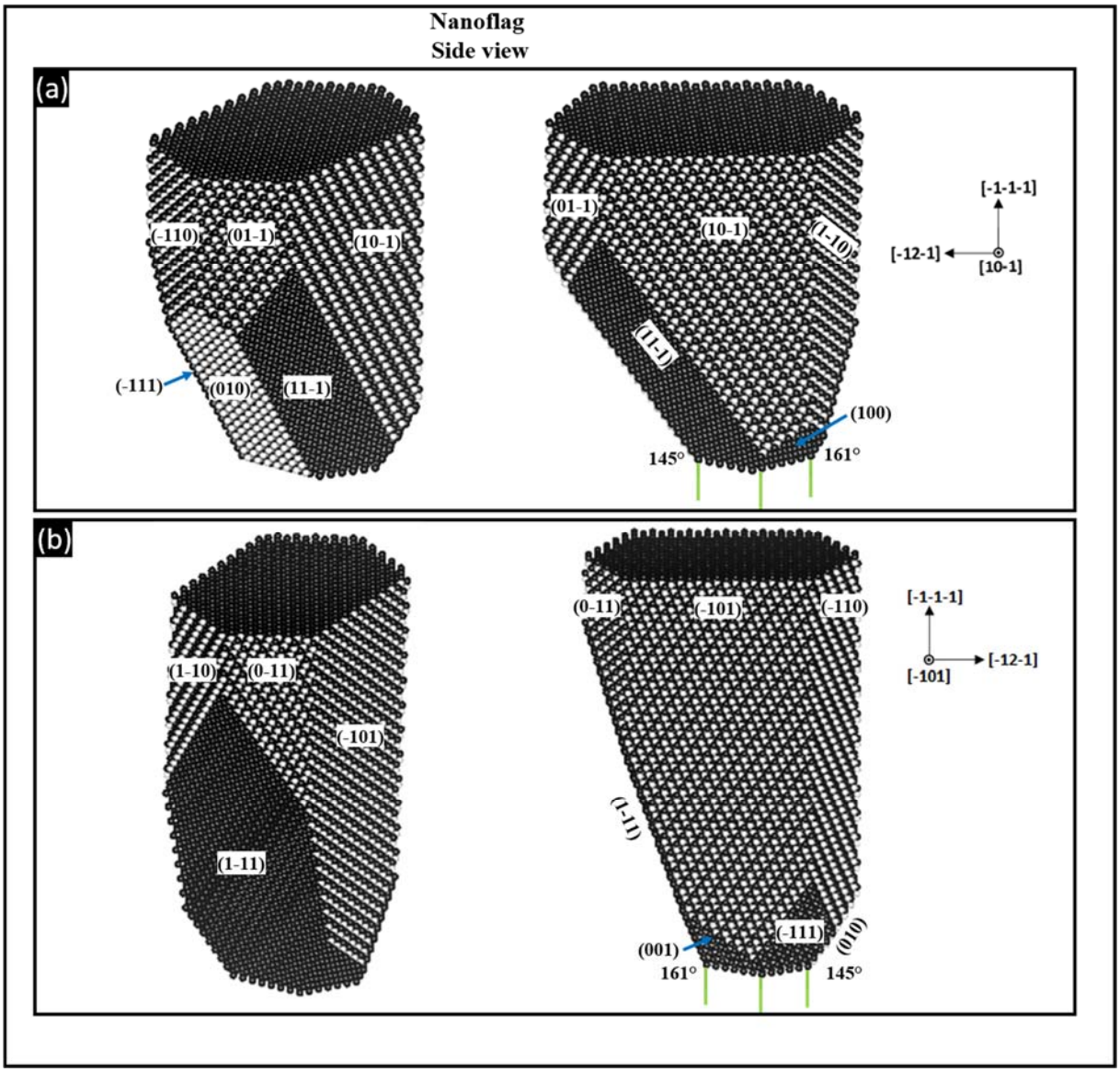

Figure S7. A 3D atomic model representing NF facets and geometry with aperture angle of 145° (a) and 160° (b).

From the combination of tilted and top view SEM and TEM images, a precise 3D atomic model was built. Statistically, we have two kinds of InSb NFs as discussed- with the apeture angle of 145° and 160°. The different structure arises due to a rotation of the InSb lattice. The faceting is visualised in side-view.